Applied Mathematics & Information Sciences **2**(1) (2008), 103–121
– An International Journal

Peristaltic Flow through a Porous Medium in an Annulus: Application of an Endoscope

Kh.S. Mekheimer[1]* and Y. Abd Elmaboud[2]

[1]Mathematics Department, Faculty of Science, Al-Azhar University, Nasr City, 11884 Cairo, Egypt

E-mail address: kh_mekheimer@yahoo.com (Kh.S. Mekheimer)

[2]Mathematics Department, Faculty of Science, Al-Azhar University (Assuit Branch), Assuit, Egypt

E-mail address: yass_math@yahoo.com (Y. Abd elmaboud)

Received May 15, 2007; Accepted August 11, 2007

Peristaltic transport with long wavelength approximation and low Reynolds number assumptions through a porous medium in an annulus filled with an incompressible viscous and Newtonian fluid, is investigated theoretically. The inner tube is uniform, rigid, while the outer tube has a sinusoidal wave traveling down its wall. The flow is investigated in a wave frame of reference moving with velocity of the wave. The velocities and the pressure gradients have been obtained in terms of the dimensionless flow rate $\overline{Q}$, the amplitude ratio ϕ, permeability of the porous medium K and the radius ratio ϵ (the ratio between the radius of the inner tube and the radius of the outer). The effects of porous medium and an endoscope on the velocities, pressure gradient, pressure rise and frictional forces on the inner and outer tubes are discussed.

Keywords: Peristaltic flow, endoscope, porous medium, pressure rise.

1 Introduction

Peristaltic pumping is a form of fluid transport that occurs when a progressive wave of area contraction or expansion propagates along the length of distensible duct. Peristalsis is an inherent property of many biological systems having smooth muscle tubes which transports biofluids by its propulsive movements and is found in the transport of urine from kidney to the bladder, the movement of chyme in the gastro-intestinal tract, intra-uterine fluid motion, vasomotion of the small blood vessels and in many other glandular ducts.

*Corresponding author

The mechanism of peristaltic transport has been exploited for industrial applications like sanitary fluid transport, blood pumps in heart lung machine and transport of corrosive fluids where the contact of the fluid with the machinery parts is prohibited. A number of analytical [1-10], numerical and experimental [11-16] studies of peristaltic flows of different fluids have been reported. there are many examples of natural porous media, such as beach sand, rye bread, wood, filter paper, human lung, etc. A good biological example of a porous medium is the pathological situation of gallstones when they fall down into bile ducts and close them partially or completely. Physiologically, inflammation of the gallbladder epithelium often results from low-grade chronic infection, and this changes the absorptive characteristics of the gallbladder mucous. As a result, cholesterol begins to precipitate, usually forming many small crystals of cholesterol on the surface of the inflamed mucous membrane. These, in turn, act as nodes for further precipitation of cholesterol, and the crystals grow larger. When such crystals fall down the common bile duct they cause loss of hepatic secretions to the gut, and also cause severe pain in the gallbladder region as well (Arthur and Guyton [17]).

Flow through a porous medium has been of considerable interest in recent years, number of workers employing Darcy's law, Rapits et al. [18], and Varshney [19] have solved problems of the flow of a viscous fluid through a porous medium bounded by a vertical surface. Mekheimer and Al-Arabi [20], studied nonlinear peristaltic transport of MHD flow through a porous medium and Mekheimer [6] studied nonlinear peristaltic transport through a porous medium in an inclined planar channel. The aim of the present study is to investigate fluid mechanics effects of peristaltic transport through a porous medium in gap between two coaxial tubes, filled with incompressible Newtonian fluid, the inner tube is rigid and the outer one have a wave trains moving independently. A motivation of the present analysis is the hope that such a problem will be applicable in many clinical applications such as the endoscope problem.

2 Formulation of the Problem

Consider creeping flow of an incompressible Newtonian fluid through coaxial tubes the gap between them filled with an isotropic porous medium. The inner tube is rigid and the outer have a sinusoidal wave traveling down its walls. The geometry of the wall surface is described in Fig. 2.1, the equations for the radii are

$$r_1' = a_1, \tag{2.1}$$

$$r_2' = a_2 + b\cos\frac{2\pi}{\lambda}(Z' - ct'), \tag{2.2}$$

where a_1, a_2 are the radius of the inner and the outer tubes, b is the amplitude of the wave, λ is the wavelength, c is the propagation velocity and t' is the time.

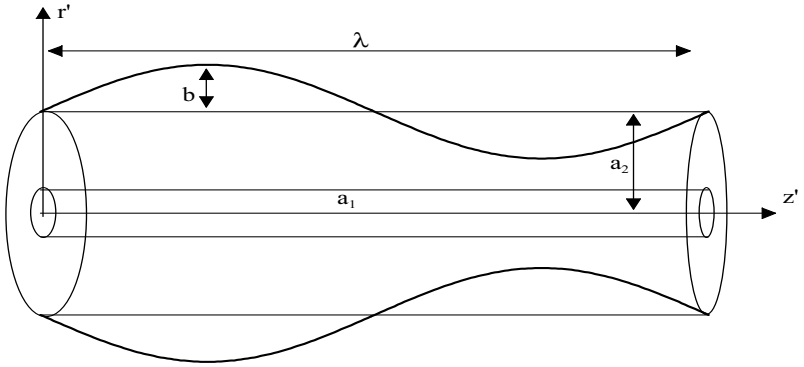

Figure 2.1: Geometry of the problem

Introducing a wave frame (r', z') moving with velocity c away from the fixed frame (R', Z') by the transformation

$$z' = Z' - ct, \quad r' = R, \quad w' = W' - c, \quad u' = U', \tag{2.3}$$

where (u', w') and (U', W') are velocity components. After using these transformation then the equations of motion are

$$\frac{\partial u'}{\partial r'} + \frac{\partial w'}{\partial z'} + \frac{u'}{r'} = 0, \tag{2.4}$$

$$\rho\left[u'\frac{\partial u'}{\partial r'} + w'\frac{\partial u'}{\partial z'}\right] = -\frac{\partial p'}{\partial r'} + \mu\left[\frac{\partial^2 u'}{\partial r'^2} + \frac{1}{r'}\frac{\partial u'}{\partial r'} + \frac{\partial^2 u'}{\partial z'^2} - \frac{u'}{r'^2}\right] - \frac{\mu}{K'}u', \tag{2.5}$$

$$\rho\left[u'\frac{\partial w'}{\partial r'} + w'\frac{\partial w'}{\partial z'}\right] = -\frac{\partial p'}{\partial z'} + \mu\left[\frac{\partial^2 w'}{\partial r'^2} + \frac{1}{r'}\frac{\partial w'}{\partial r'} + \frac{\partial^2 w'}{\partial z'^2}\right] - \frac{\mu}{K'}(w' + c), \tag{2.6}$$

where u' and w' are the velocity components in the r' and z' directions, respectively, ρ is the density, p' is the pressure, μ is the viscosity, and K' permeability of the porous medium. We introduce the following nondimensional variables

$$\begin{gathered} r = \frac{r'}{a_2},\ z = \frac{z'}{\lambda},\ w = \frac{w'}{c},\ u = \frac{\lambda u'}{a_2 c},\ p = \frac{a_2^2}{\lambda\mu c}p',\ K = \frac{K'}{a_2^2}, \\ r_1 = \frac{r_1'}{a_2} = \epsilon, \quad r_2 = \frac{r_2'}{a_2} = 1 + \phi\cos(2\pi z), \\ Re = \frac{\rho c a_2}{\mu},\ \ \delta = \frac{a_2}{\lambda},\ \ \epsilon = \frac{a_1}{a_2}, \end{gathered} \tag{2.7}$$

where ϕ is the amplitude ratio, Reynolds number Re and δ is the dimensionles wave number.

To proceed, we non-dimensionalize Eqs. (2.4-2.6), this yields

$$\frac{1}{r}\frac{\partial(ru)}{\partial r} + \frac{\partial w}{\partial z} = 0, \tag{2.8}$$

$$Re\delta^3\left[u\frac{\partial u}{\partial r}+w\frac{\partial u}{\partial z}\right]=-\frac{\partial p}{\partial r}+\delta^2\frac{\partial}{\partial r}\left(\frac{1}{r}\frac{\partial(ru)}{\partial r}\right)+\delta^4\frac{\partial^2 u}{\partial z^2}-\frac{\delta^2}{K}u, \tag{2.9}$$

$$Re\delta\left[u\frac{\partial w}{\partial r}+w\frac{\partial w}{\partial z}\right]=-\frac{\partial p}{\partial z}+\frac{1}{r}\frac{\partial}{\partial r}\left(r\frac{\partial w}{\partial r}\right)+\delta^2\frac{\partial^2 w}{\partial z^2}-\frac{1}{K}(w+1). \tag{2.10}$$

Using the long wavelength approximation and dropping terms of order δ and higher, it follows from Eqs. (2.8-2.10) that the appropriate equations describing the flow in the wave frame are

$$\frac{1}{r}\frac{\partial(ru)}{\partial r}+\frac{\partial w}{\partial z}=0, \tag{2.11}$$

$$\frac{\partial p}{\partial r}=0, \tag{2.12}$$

$$\frac{\partial p}{\partial z}=\frac{1}{r}\frac{\partial}{\partial r}\left(r\frac{\partial w}{\partial r}\right)-\frac{1}{K}(w+1), \tag{2.13}$$

Eq.(2.12) shows that p is not a function of r. The corresponding dimensionless boundary conditions are

$$\begin{aligned} w&=-1 \qquad at \qquad r=r_1,\\ w&=-1 \qquad at \qquad r=r_2. \end{aligned} \tag{2.14}$$

The expressions for the velocity profile of the fluid, obtained as the solutions of Eqs.(2.13) subject to the boundary conditions (2.14) are given as

$$w(r,z)=I_0(mr)\left(\frac{b_{11}p_z}{m^2b_{13}}\right)+K_0(mr)\left(\frac{b_{12}p_z}{m^2b_{13}}\right)-\frac{(m^2+p_z)}{m^2}, \tag{2.15}$$

where

$$m=\frac{1}{\sqrt{K}}\ ,\quad b_{11}=K_0(mr_1)-K_0(mr_2),\quad b_{12}=I_0(mr_2)-I_0(mr_1),$$

$$b_{13}=I_0(mr_2)K_0(mr_1)-I_0(mr_1)K_0(mr_2).$$

where I_0, K_0 are the modified Bessel function of the first and second kind respectively of order 0. The velocity $u(r,z)$ can be obtained from Eq.(2.11) after using Eq.(2.15), we get

$$\begin{aligned} u(r,z)=&\frac{1}{2m^4b_{13}^2rr_2}\Big[2p_zr_2'\big(mr(I_1(mr)K_0(mr_1)+I_0(mr_1)K_1(mr))-1\big)(mr_2b_{16}-1)\\ &+r_2p_z'b_{13}\{2+m(mK_0(mr_2)\big[r_1^2I_2(mr_1)-r^2I_0(mr_1)\big]-2b_{11}rI_1(mr)\\ &-2rI_0(mr_1)K_1(mr)+I_0(mr_2)\big(mr^2K_0(mr_1)+2rK_1(mr)\\ &-mr_1^2K_2(mr_1)\big))\}\Big], \end{aligned} \tag{2.16}$$

where

$$b_{14}=I_0(mr_2)K_2(mr_1)-I_2(mr_1)K_0(mr_2),$$

$$b_{15}=I_0(mr_1)K_2(mr_2)-I_2(mr_2)K_0(mr_1),$$

$$b_{16} = I_1(mr_2)K_0(mr_1) + I_0(mr_1)K_1(mr_2),$$

and the prime ($'$) denotes differentiation w.r.t z. The corresponding stream function ($u = -(1/r)\partial\psi/\partial z$ and $w = (1/r)\partial\psi/\partial r$) is

$$\begin{aligned}\psi(r,z) =&\{m^4 b_{13}(r_1^2 - r^2) + p_z[-2 + m(2rb_{11}I_1(mr) + mK_0(mr_2)(r^2 I_0(mr_1)\\ &- r_1^2 I_2(mr_1)) + 2rI_0(mr_1)K_1(mr) + I_0(mr_2)(mr_1^2 K_2(mr_1)\\ &- r(mrK_0(mr_1) + 2K_1(mr))))]\} \times \frac{1}{2m^4 b_{13}}. \end{aligned} \tag{2.17}$$

The instantaneous volume flow rate $Q(z)$ is given by

$$Q(z) = 2\int_{r_1}^{r_2} rw(r,z)dr = (r_1^2 - r_2^2) + \frac{p_z}{m^4 b_{13}}\left[m^2(b_{14}r_1^2 + b_{15}r_2^2) - 4\right], \tag{2.18}$$

From Eq.(2.18) we get

$$p_z = \frac{m^4 b_{13}}{[m^2(b_{14}r_1^2 + b_{15}r_2^2) - 4]} \times \left(Q(z) - (r_1^2 - r_2^2)\right). \tag{2.19}$$

Following the analysis given by Shapiro et al.[1], the mean volume flow, $\overline{Q}$ over a period is obtained as

$$\overline{Q} = Q(z) + (1 + \frac{\phi^2}{2}) - \epsilon^2, \tag{2.20}$$

which on using Eq.(2.19) yields

$$p_z = \frac{m^4 b_{13}}{[m^2(b_{14}r_1^2 + b_{15}r_2^2) - 4]} \times \left(\overline{Q} + \epsilon^2 - (1 + \frac{\phi^2}{2}) - (r_1^2 - r_2^2)\right). \tag{2.21}$$

The pressure rise Δp and the friction force (at the wall) on the outer and inner tubes are $F^{(o)}$ and $F^{(i)}$ respectively, in a tube of length L, in their non-dimensional forms, are given by

$$\Delta p = \int_0^1 p_z dz, \tag{2.22}$$

$$F^{(o)} = \int_0^1 r_2^2(-p_z)dz, \tag{2.23}$$

$$F^{(i)} = \int_0^1 r_1^2(-p_z)dz. \tag{2.24}$$

Substituting from Eq.(2.21) in Eqs.(2.22 -2.24) with $r_1 = \epsilon, \quad r_2 = 1 + \phi\cos(2\pi z)$, we get the pressure rise and the friction force (at the wall) on the outer and inner tubes.

In the absence of the porous medium and the inner tube ($i.e., K \to \infty, r_1 = 0$), the pressure rise and the outer friction force in this case take the form

$$\Delta p = \frac{-8}{(1-\phi^2)^{7/2}}\left\{\overline{Q}\left(1 + \frac{3}{2}\phi^2\right) + \frac{\phi^2}{4}(\phi^2 - 16)\right\}, \tag{2.25}$$

$$F^{(o)} = \frac{8}{(1-\phi^2)^{3/2}} \left\{ \overline{Q} - 1 - \frac{\phi^2}{2} + (1-\phi^2)^{3/2} \right\}. \tag{2.26}$$

The results obtained in Eqs.(2.25-2.26) are the same as those obtained by Shapiro et al.[1].

3 Numerical Results and Discussion

In order to have an estimate of the quantitative effects of the various parameters involved in the results of the present analysis we using the MATHEMATICA program. The numerical evaluations of the analytical results obtained for Δp, $F^{(o)}$, $F^{(i)}$, for different parameters values [20-23]: $\epsilon = 0.32$ up to 0.44, $L = \lambda = 8.01$ cm, and $K = 0.05$ up to 0.5.

In Fig. 3.1 the variation of $\frac{dp}{dz}$ versus z is shown for different values of K and $\overline{Q}$ by fixing the other parameters $\epsilon = 0.32$ (endoscope problem) and $\phi = 0.4$, it is notice that the maximum amplitude of the pressure gradient $\frac{dp}{dz}$ decreases as K and $\overline{Q}$ increase. The effect of changing the amplitude ratio ϕ and radius ratio ϵ is indicated in Fig. 3.2, we observe that there is an increase in the maximum amplitude of $\frac{dp}{dz}$ when increasing ϕ and ϵ.

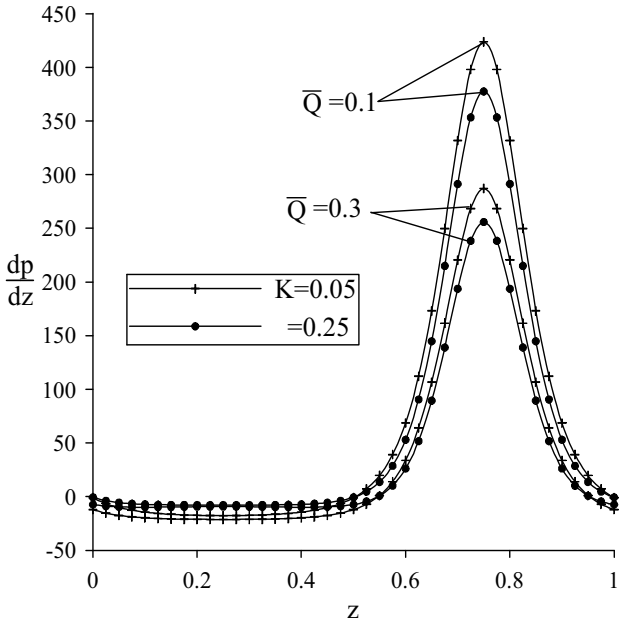

Figure 3.1: The variation of pressure gradient $\frac{dp}{dz}$ with z for different values of K and $\overline{Q}$ at $\epsilon = 0.32$, $\phi = 0.4$.

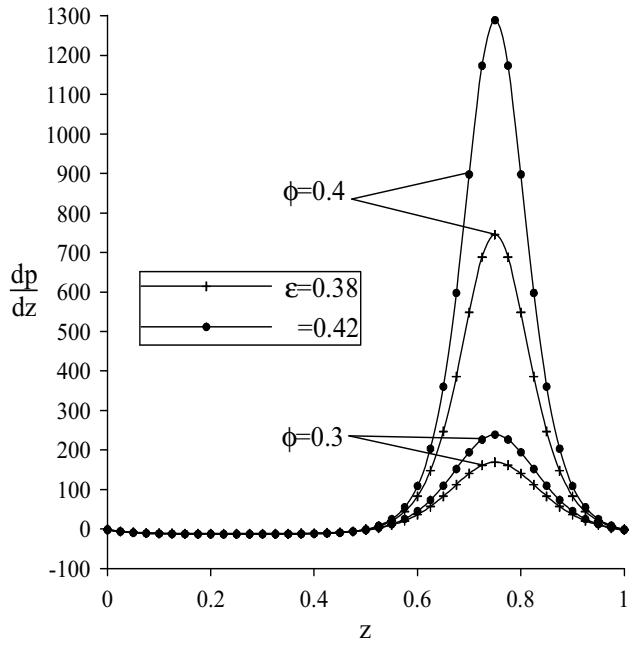

Figure 3.2: The variation of pressure gradient $\frac{dp}{dz}$ with z for different values of ϵ and ϕ at $K = 0.1$, $\overline{Q} = 0.1$.

It is evident from Fig. 3.3 that there is linear relation between pressure rise and flow rate, also an increase in the flow rate reduces the pressure rise and thus maximum flow rate is achieved at zero pressure rise and maximum pressure occurs at zero flow rate. The pressure rise decreases as K increases but it increases as ϵ increase.
Fig. 3.4, depicts the variation of Δp with $\overline{Q}$ at $\epsilon = 0.32$, for different values of amplitude ratio ϕ and K. An interesting observation here is that the pressure rise increases with increase ϕ. The pumping regions, peristaltic pumping ($\overline{Q} > 0$ and $\Delta p > 0$), augmented pumping ($\overline{Q} > 0$ and $\Delta p < 0$) and retrograde pumping ($\overline{Q} < 0$ and $\Delta p > 0$) are also shown in Figs. 3.3-3.4 and it is clear that the peristaltic pumping region becomes wider as the radius ratio ϵ, amplitude ratio ϕ increases.

The variation of Δp with permeability of the porous medium K for different values flow rate $\overline{Q}$ and radius ratio ϵ at $\phi = 0.4$ is presented in Fig. 3.5. It is observed that the relation between Δp and K is non linear relation, Δp decreases with increase K.

Figs. 3.6 and 3.7 describe the results obtained for the inner friction $F^{(i)}$ versus the flow rate $\overline{Q}$ and Fig. 3.8 depicts the variation of inner friction $F^{(i)}$ versus permeability of the porous medium K.

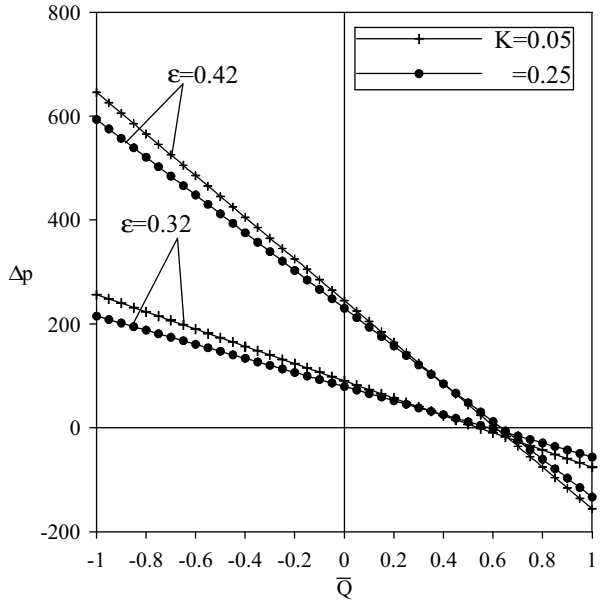

Figure 3.3: The variation of Δp with $\overline{Q}$ for different values of K and ϵ at $\phi = 0.4$.

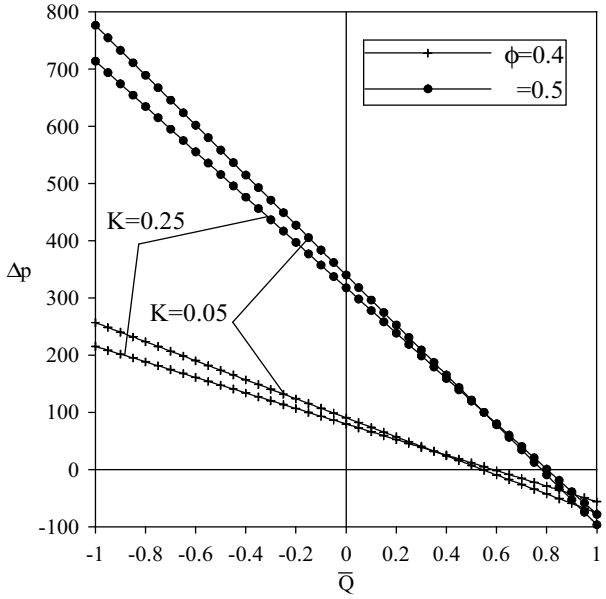

Figure 3.4: The variation of Δp with $\overline{Q}$ for different values of ϕ and K at $\epsilon = 0.32$.

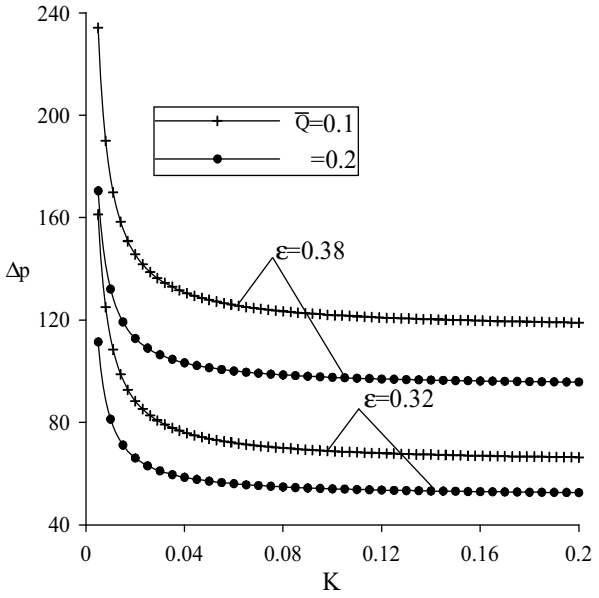

Figure 3.5: The variation of Δp with K for different values of $\overline{Q}$ and ϵ at $\phi = 0.4$.

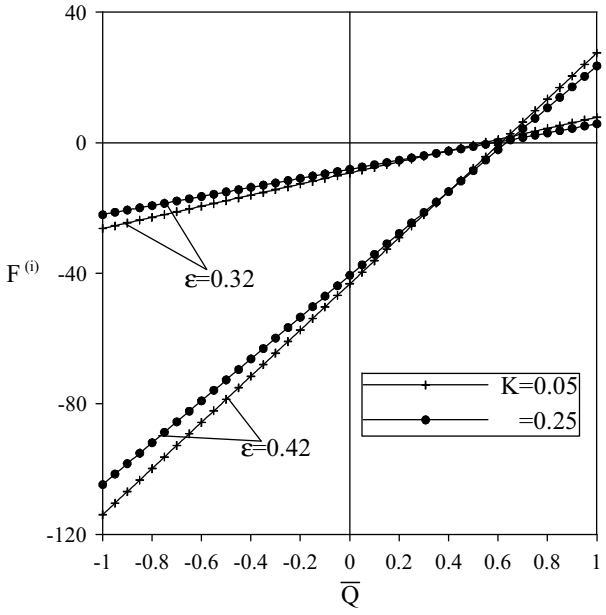

Figure 3.6: The variation of $F^{(i)}$ with $\overline{Q}$ for different values of K and ϵ at $\phi = 0.4$.

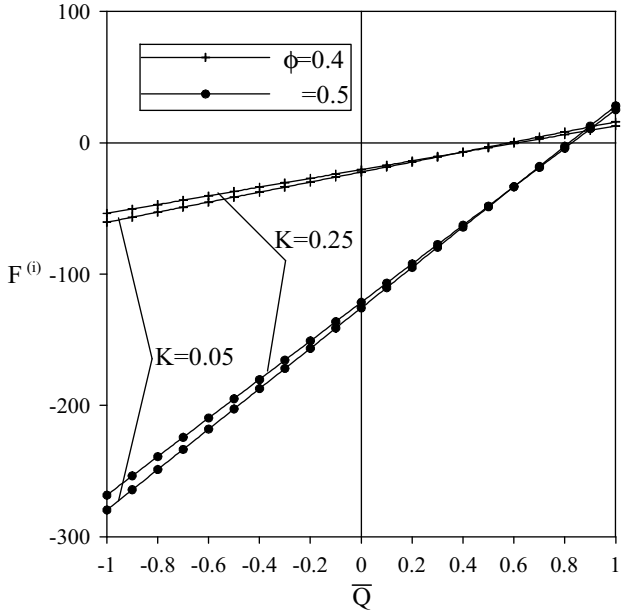

Figure 3.7: The variation of $F^{(i)}$ with $\overline{Q}$ for different values of K and ϕ at $\epsilon = 0.38$.

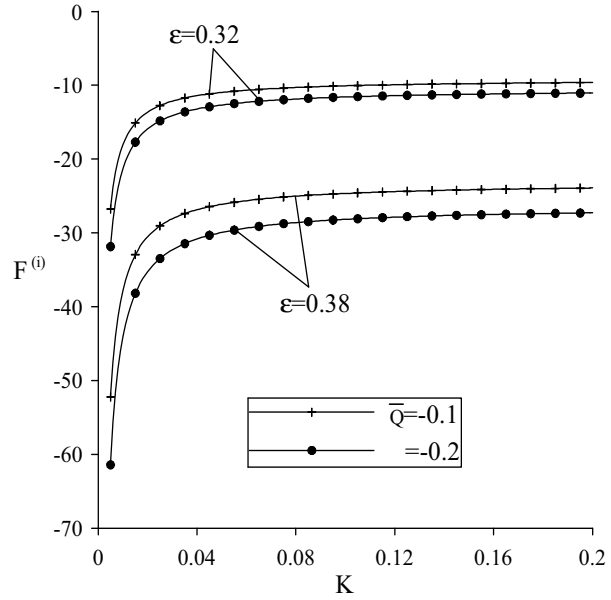

Figure 3.8: The variation of $F^{(i)}$ with K for different values of $\overline{Q}$ and ϵ at $\phi = 0.4$.

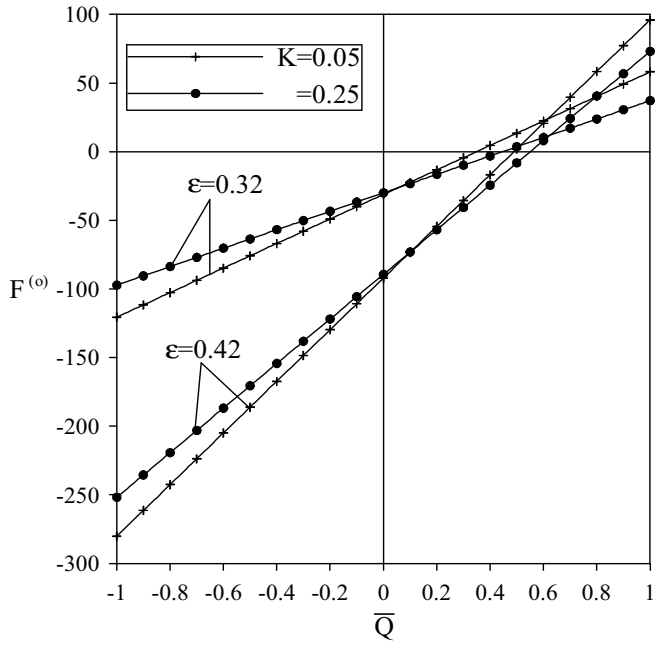

Figure 3.9: The variation of $F^{(o)}$ with $\overline{Q}$ for different values of K and ϵ at $\phi = 0.4$.

Figs. 3.9 and 3.10 describe the results for outer friction force $F^{(o)}$ versus the flow rate $\overline{Q}$ and Fig. 3.11 depicts the variation of outer friction $F^{(o)}$ versus permeability of the porous medium K.

Furthermore, the effect of important parameters as $\overline{Q}$, K, ϵ and ϕ on the inner and outer friction force have been investigated.

We notice from these figures that the inner and outer friction force have the opposite behavior compared to the pressure rise. The inner friction force behaves similar to the outer friction force for the same values of the parameters, moreover the outer friction force is greater than the inner friction force at the same values of the parameters.

The effect of the permeability of the porous medium K on the contour map of the velocities $w(r, z)$ and $u(r, z)$ are investigated in Figs. 3.12 and 3.13. The lighter colored regions have a higher velocity than the regions shaded darker. Fig. 3.12 shows that the velocity w, increases as permeability of the porous medium K increases also the height and the width of the bolus decreases. The behavior of the streamlines near the walls are same as the walls. Fig. 3.13 shows that the velocity u. It is notice that a steepening of the edges in the sinusoidal behavior of u. There is an increase in the size of the bolus as permeability of the porous medium K increase.

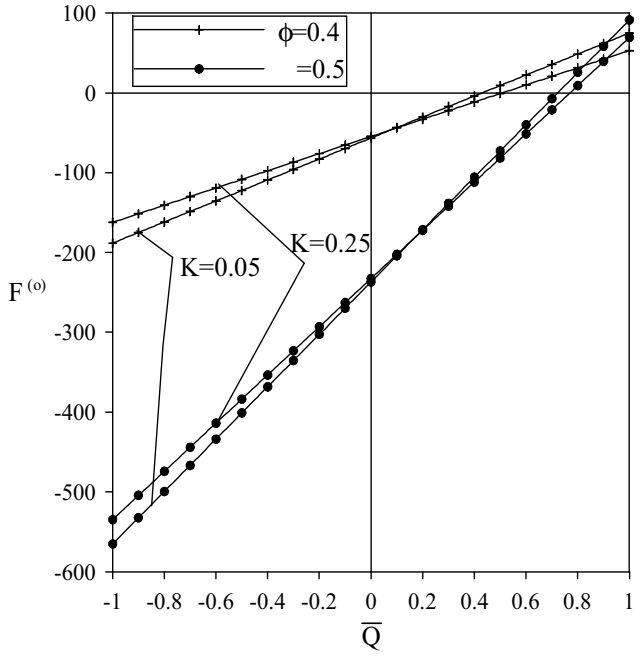

Figure 3.10: The variation of $F^{(o)}$ with $\overline{Q}$ for different values of ϕ and K at $\epsilon = 0.38$.

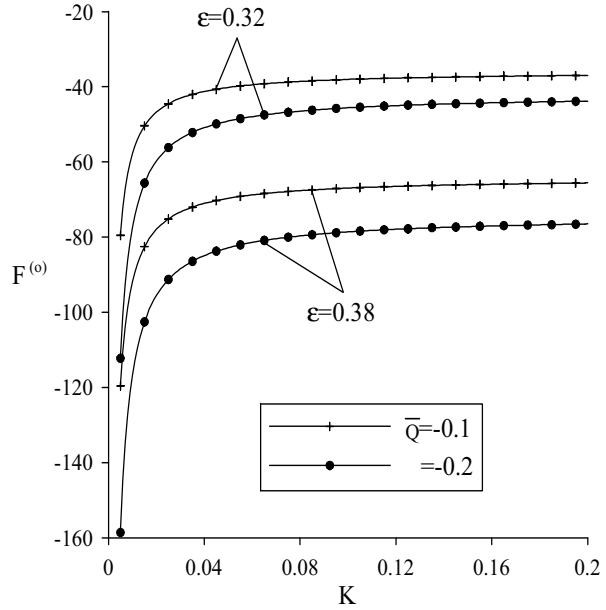

Figure 3.11: The variation of $F^{(o)}$ with K for different values of $\overline{Q}$ and ϵ at $\phi = 0.4$.

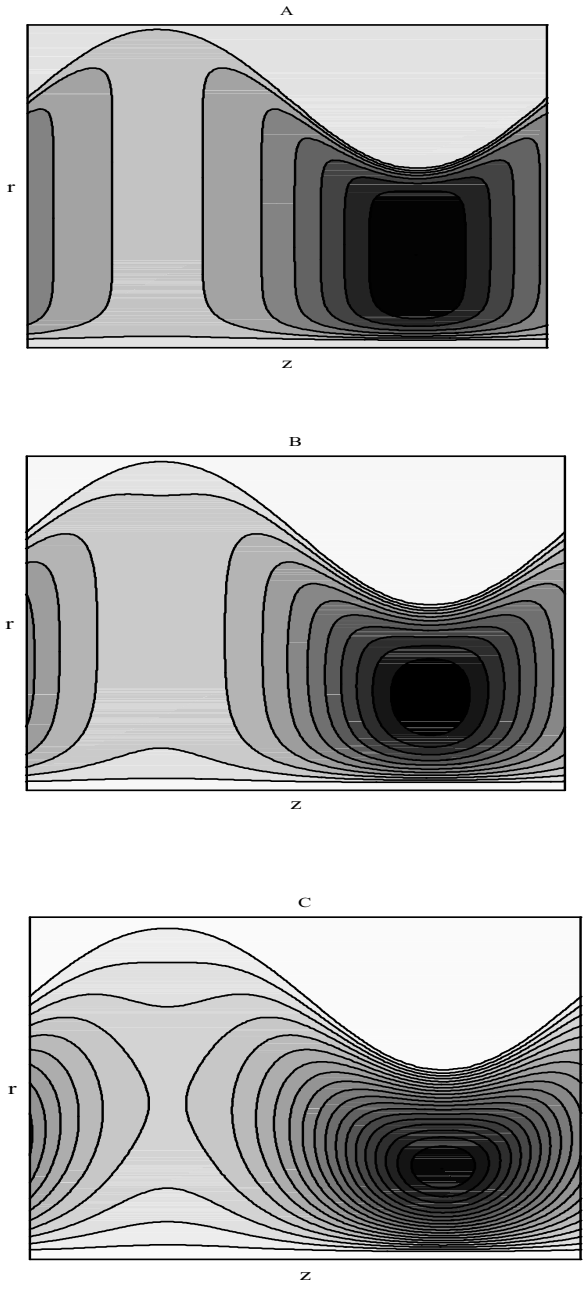

Figure 3.12: The contour plot for the velocity $w(r, z)$ at $\overline{Q} = -1$, $\epsilon = 0.32$, $\phi = 0.2$ with $(A)K = 0.001$, $(B)\ K = 0.005$, $(C)\ K = 0.5$, $r \in [\epsilon, r_2(z)]$ and $z \in [0, 1]$.

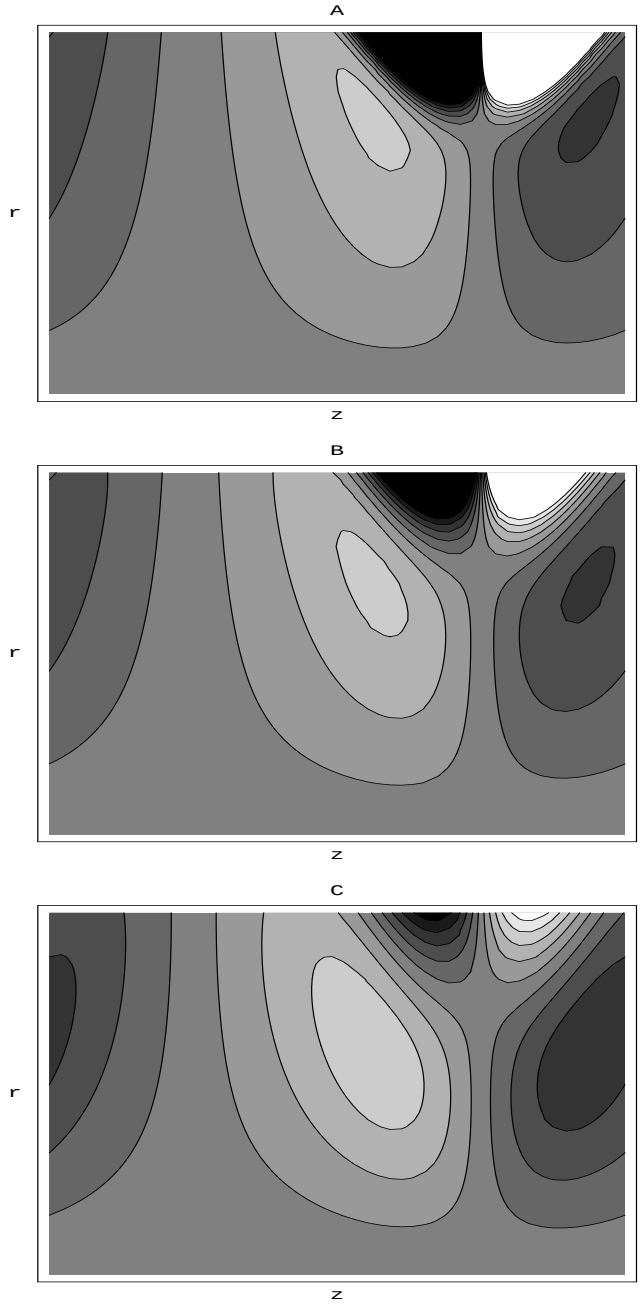

Figure 3.13: The contour plot for the velocity $u(r,z)$ at $\overline{Q}=-1$, $\epsilon=0.32$, $\phi=0.2$ with $(A)K=0.001$, (B) $K=0.005$, (C) $K=0.5$, $r\in[\epsilon,r_2(z)]$ and $z\in[0,1]$.

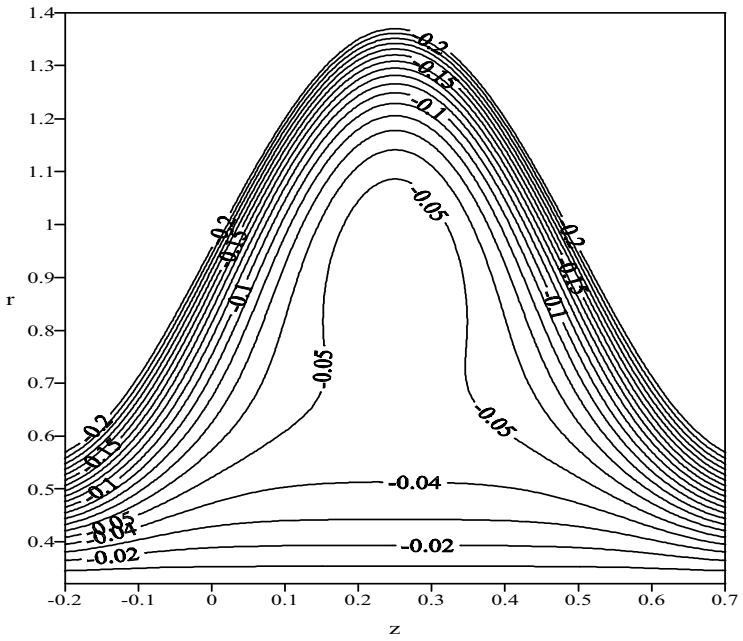

Figure 3.14: Graph of the streamlines for $\overline{Q} = 0.5$, $\epsilon = 0.32$, $\phi = 0.4$ and $K = 0.05$.

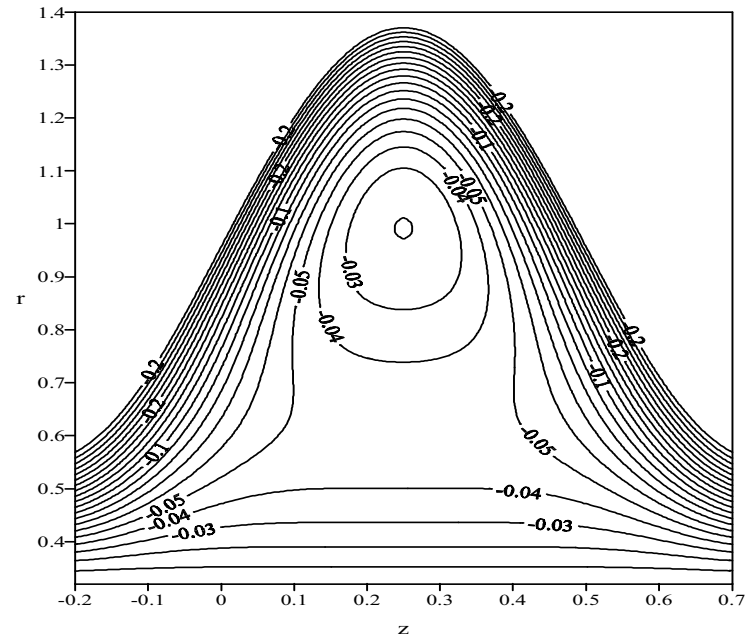

Figure 3.15: Graph of the streamlines for $\overline{Q} = 0.5$, $\epsilon = 0.32$, $\phi = 0.4$ and $K = 0.9$.

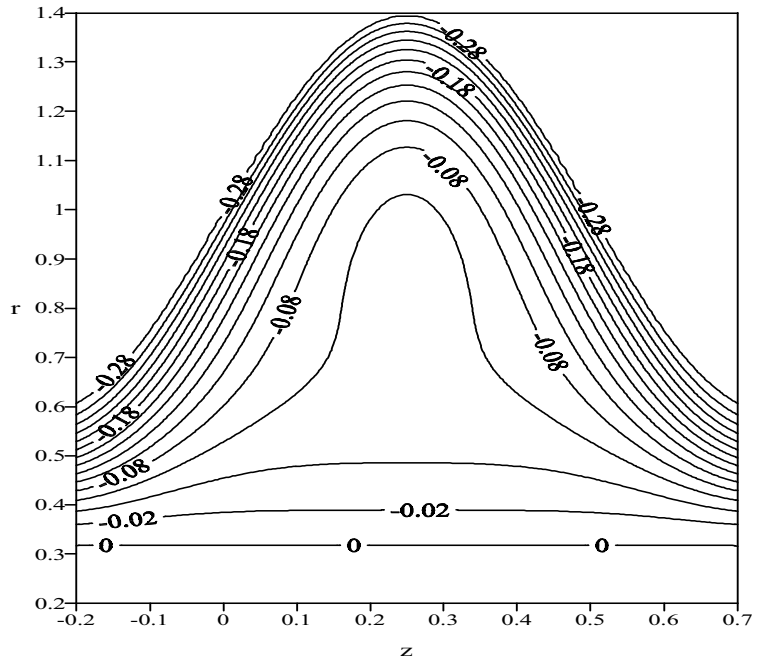

Figure 3.16: Graph of the streamlines for $\overline{Q} = 0.1$, $\epsilon = 0.32$, $\phi = 0.4$ and $K = 0.2$.

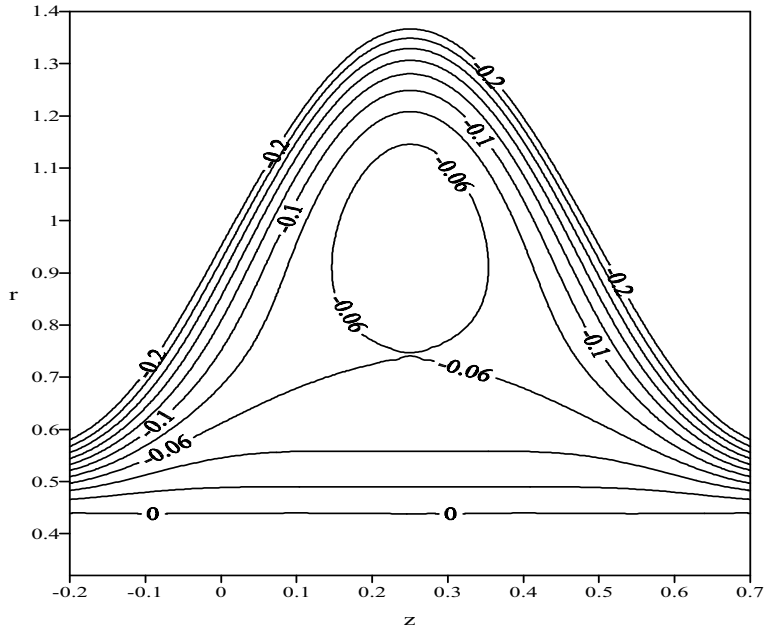

Figure 3.17: Graph of the streamlines for $\overline{Q} = 0.1$, $\epsilon = 0.44$, $\phi = 0.4$ and $K = 0.2$.

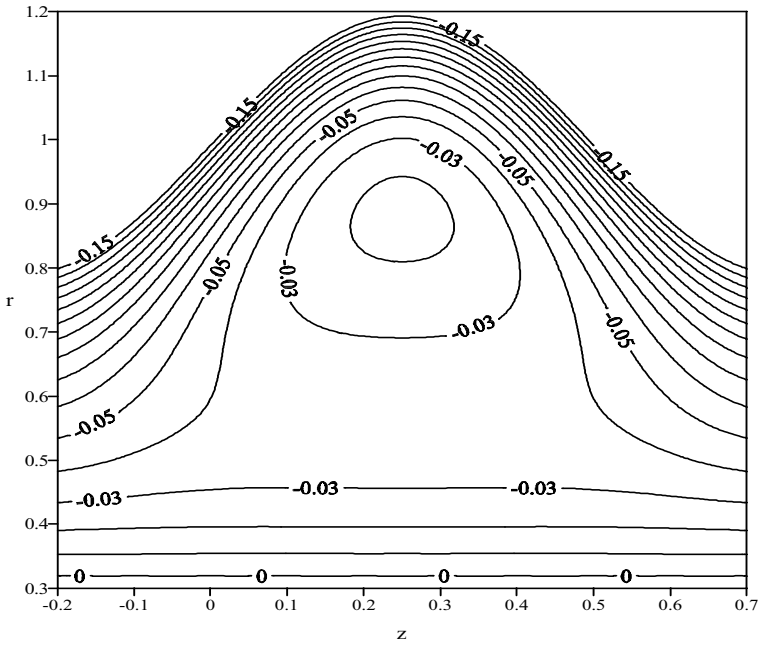

Figure 3.18: Graph of the streamlines for $\overline{Q} = 0.6$, $\epsilon = 0.32$, $\phi = 0.2$ and $K = 0.1$.

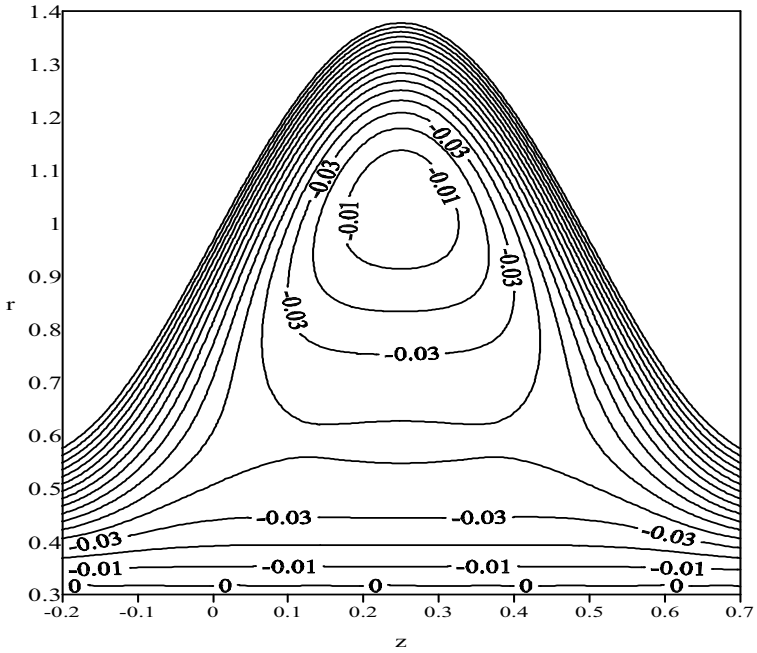

Figure 3.19: Graph of the streamlines for $\overline{Q} = 0.6$, $\epsilon = 0.32$, $\phi = 0.4$ and $K = 0.1$.

4 Streamlines and Fluid Trapping

The phenomenon of trapping, whereby a bolus (defined as a volume of fluid bounded by a closed streamlines in the wave frame) is transported at the wave speed. Figs. 3.14 and 3.15 illustrate the streamline graphs for different values of permeability of the porous medium K for other given fixed set of parameters. It is observed that the permeability of the porous medium increases the velocities which lead to the fluid element spin forms bolus this indicate that the bolus appears as K increases.

The effects of the radius ratio ϵ on the trapping are illustrated in Figs. 3.16-3.17. It is evident that the the streamlines near the walls are parallel to the walls when radius ratio ϵ is small but by increasing the radius ratio the bolus appearing. The effects of the amplitude ratio ϕ on the trapping are illustrated in Figs. 3.18-3.19. It is evident that the size of trapping bolus increases with increases ϕ with fixing other parameters.

References

[1] A.H. Shapiro, M.Y. Jaffrin, S.L. Weinberg, Peristaltic pumping with long wavelengths at low Reynolds number, *J. Fluid Mech.* **37** (1969), 799–825.

[2] T.F. Zien and S.A. Ostrach, A long wave approximation to peristaltic motion, *J. Biomech.* **3** (1970), 63–75.

[3] E.F. El Shehawey and Kh.S. Mekheimer, Couple-stresses in peristaltic transport of fluids, *J. Phys. D: Appl. Phys.* **27** (1994), 1163–1170.

[4] R.A Ramachandra and S. Usha, Peristaltic transport of two immiscible viscous fluids in a circular tube, *J. Fluid Mech.* **298** (1995), 271–285.

[5] Kh.S. Mekheimer, E.F. El Shehawey, A.M. Elaw, Peristaltic motion of a particle-fluid suspension in a planar channel, *Int. J. Theor. Phys.* **37** (1998), 2895–2919.

[6] Kh.S. Mekheimer, Non-linear peristaltic transport through a porous medium in an inclined planar channel, *J. Porous Medium* **6** (2003), 189–201.

[7] Kh.S. Mekheimer, Peristaltic transport of a couple-stress fluid in a uniform and non-uniform channels, *Biorheology*, **39** (2002),755–765.

[8] Kh.S. Mekheimer, Non-linear peristaltic transport of magneto-hydrodynamic flow in an inclined planar channel, *AJSE* **28** (2003), 183–201.

[9] K. Vajravelu, S. Sreenadh and V. R. Babu, Peristaltic transport of a Herschel-Bulkley fluid in an inclined tube, *International Journal of Non-Linear Mechanics* **40** (2005) 83–90.

[10] Abd El Hakeem Abd El Naby, A. E. M. El Misery and M. F. Abd El Kareem, Effects of a magnetic field on trapping through peristaltic motion for generalized Newtonian fluid in channel, *Physica A* **367** (2006) 79–92.

[11] T. W. Latham, *Fluid Motion in a Peristaltic Pump*, M.Sc. Thesis, MIT, Cambridge, MA, 1966.

[12] S. Takabatake and K. Ayukawa, Numerical study of two dimensional peristaltic flows, *J. Fluid Mech.* **122** (1982) 439–465.

[13] S. Takabatake, K. Ayukawa and A. Mori, Peristaltic pumping in circular cylindrical tubes: a numerical study of fluid transport and its efficiency, *J. Fluid Mech.* **193** (1988) 267–233.

[14] D. Tang and M. Shen, Non-stationary peristaltic and transport of a heat-conducting fluid, *J. Math. Anal. Appl.* **174** (1993) 265–289.

[15] T.D. Brown and T. K. Hung, Computational and experimental investigations of two-dimensional nonlinear peristaltic flows, *J. Fluid Mech.* **83** (1977), 249–272.

[16] B. V. Rathish Kumar and K. B. Naidu, A numerical study of peristaltic flows, *Computers and Fluids* **24** (1995), 161–176.

[17] C. Arthur and M. D. Guyton, *Medical physiolgy*, 7th edn., W.B. Saunders Company 1992.

[18] A. Rapits, N. Kafousias and C. Massalas, Free Convection and mass transfer flow through a porous medium bounded by an infinite vertical porous plate with constant heat flux, *Z. Angew. Math. Mech.* **62** (1982), 489–491.

[19] C. L. Varshney, The fluctuating flow of a viscous fluid through a porous medium bounded by a porous and horizontal surface, *Indian J. Pure Appl. Math.* **10** (1979), 1558–1572.

[20] Kh.S. Mekheimer and T.H. Al-Arabi, Nonlinear peristaltic transport of MHD flow through a porous medium, *International J. of mathematics and mathematical sciences* **26** (2003), 1663–1682.

[21] Kh. S. Mekheimer, Peristaltic transport of a Newtonian fluid through a uniform and non-uniform annulus, *The Arabian J. for Sc. and Eng.* **30** (2005), 69–73.

[22] Abd El Hakeem Abd El Naby, A. E. M. El Misery and I. I. El Shamy, Effects of an endoscope and fluid with variable viscosity on peristaltic motion, *Applied Mathematics and Computation* **158** (2004), 497–511.

[23] T. Hayat, N. Ali, S. Asghar and A. M. Siddiqui, Exact peristaltic flow in tubes with an endoscope, *Applied Mathematics and Computation* **182** (2006), 359–368.